Advances in Environment and Energies
Volume 2, Issue 1, No. 5
Received 3 March 2023; Accepted 15 May 2023
Published online 23 May 2023

Sanderman Publishing House

Influence of the temperature and the concentration of methanol on a direct methanol fuel cell

Mihoub Medkour, Toufik bensana
Laboratoire des Aéronefs, Université SAAD DAHLAB de Blida 1, Blida, Algeria.
Email: [1]*medkourmihoub1972@gmail.com*

Abstract. A one-dimensional mathematical model, which permits semi-empirical prediction of the overall performance of a direct methanol gas telephone (DMFC) has exceptional temperatures for a proton change membrane by using the usage of parameters acquired from the classical characterization techniques is presented. The strategies conventionally used are characterised as follows: the impedance spectroscopy (proton conductivity), water absorption (water absorption), the perevaporation (methanol permeability and water) and gasoline permeation experiments (permeability to oxygen, nitrogen and carbon dioxide). This mannequin was once validated experimentally the use of the outcomes got with membranes Poly (vinylidene fl uoride-hexa fluorine opropylene) (PVdF-HFP) / Nafion ionomer / aluminum oxy hydroxide organized through segment inversion method [1]. The mannequin precisely anticipated the polarization curves and DMFC overall performance in phrases of open circuit voltage and the cutting-edge density, the attention of methanol and water in accordance to the residences of the membrane effectively. This information affirm that the simulator can effectively predict the DMFC performance, the usage of the basic characterization statistics as mannequin enters parameters.

Keywords. Passive direct methanol fuel cell, modeling, methanol crossover, water crossover.

1. Introduction

The largest assignment of the twenty first century is to furnish smooth strength barring affecting the environment. The technological know-how of gas cells is recognised to be one of the key applied sciences in the power provide for stationary functions (eg, electricity flowers blocks) and cellular functions (eg, vehicles, laptops and mobilephone phones) due to the fact of its benefits such as no exclusive surroundings to work properly (other than a warmness sink) and its excessive efficacy each electric powered and bodily (without sound and with some distance much less air pollution harmful) [2]. Recently, the direct methanol gas phone (DMFC) is recognized as an choice electricity generator for transportation and transportable functions due to the fact it is such a compact plan and simplified system, it has no gas processing unit (reforming) and storage. The electrode / membrane (MEA) greatly affects the performance of fuel cells. Note that the phenomena that Inhibit the proper functioning of the cell membrane repositioning. The DMFC has a variety of parameters that affect the overall performance. These parameters are as follows: concentration of methanol, the operating temperature, the flow rate of methanol and the thickness of the membrane. By optimizing the parameters, high efficiency of DMFC can be achieved while maintaining the methanol crossover and the cross flow will be low [1-3]. The characteristics obtained for a membrane to be used as inputs into a mathematical mannequin to predict the overall performance of corresponding DMFC. So as an alternative of having solely a qualitative prediction of DMFC overall performance based totally on experimental consequences of the research, this kind of mannequin have to permit a quantitative prediction. However, most of the researches on modeling the DMFC have been worn on the Nafion® using many parameters literature [4-5]. This work focuses on the improvement of a semi-empirical mathematical mannequin to predict the overall performance of DMFC the use of incoming bought with the aid of characterization strategies such as impedance spectroscope and pervaporation. A defined change in the performance of DMFC was quantified using this membrane with different temperatures. The impact of methanol awareness on the internet water transport coefficient used to be experimentally studied with the aid of Jewett et al. [31, 32] Abdelkareem et al. [26] Zhao et al. [8], Song et al. [4] and Xu et al. [25]. Therefore, the improvement of a mathematical mannequin to predict the DMFC overall performance at regular nation imply the simulation of a broad range of residences of the bodily / chemical membrane. In summary, the motive of this finds out about in the context of growing a simulator that can successfully limit our efforts to perceive the fantastic working prerequisites for this telephone [6-5].

2. Mathematical model

So far, the mathematical fashions developed for DMFC gas cells have in fact carried on the running prerequisites of gasoline cells the usage of perfluorinated PEM membranes [7]. Unfortunately, these fashions use records from the literature, which are commonly not possible to reproduce with the aid of membrane improvement lookup agencies and in many cases, these parameters characterize the houses of the membranes beneath development, accordingly limiting the success of models. To grant a beneficial device for predicting the overall performance of DMFC for a sure subject, our work provides a unique semi-empirical mathematical mannequin for PEM DMFC the use of the homes acquired from the effects of classical characterization [2]. This mannequin is developed which is one-dimensional steady-state, comprising the multilayer shape of the MEA (Fig. 1), taking into account the multi-component service (CH3OH, H2O)

and certain electrochemical reactions. The mannequin makes use of information received from the following characterization techniques mentioned in [8]:

Pervaporation experiments:

Permeability of methanol (1) and water (2), P_1^M , P_2^M respectively.

Gas permeation experiments

Permeability of oxygen (3), carbon dioxide (4) and nitrogen (5), and P_3^M , P_4^M , P_5^M respectively.

Swelling Experience

Swelling by liquid water $S_{2,L}^M$

Impedance spectroscopy

Proton conductivity of the membrane k_M

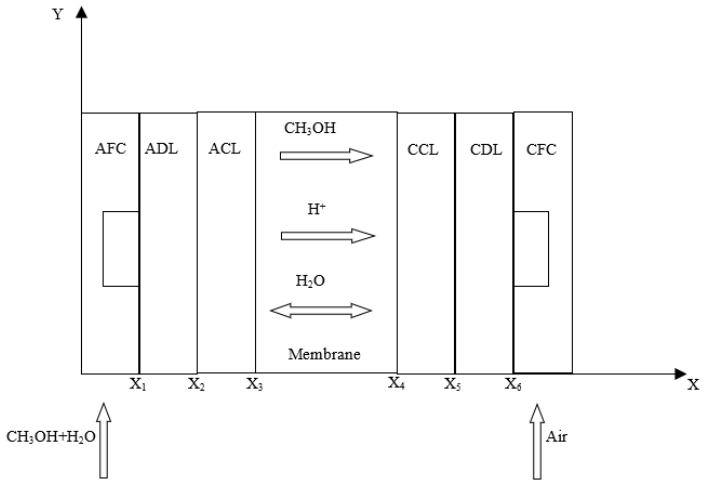

Figure 1. Schema DMFC illustrating the mass transport of species thru the membrane proton alternate gas telephone DMFC

All the parameters regarding the species transported thru the electrodes and electrochemical reactions kinetics had been taken from the literature (Table .1). The decision of diffusion equations in the layers of the anode and the cathode and the membrane are discretized into one-dimensional the usage of the finite extent approach [9]. The overall performance of experimental DMFC introduced in [1] was once used as the mannequin validation data. Transport of methanol and water in the anode and the prediction of the polarization curves, the open circuit voltage is modeled.

2.1. The mass transport

A. Anode

Anodic reaction:

Oxidation of methanol: $CH_3OH + H_2O \rightarrow CO_2 + 6H^+ + 6e^-$

The methanol transport approaches and water from the gas tank are described by:

$$N_i^{DA} = Q^{FA} C_T \left(x_i^{FA} - x_i^A \right) \tag{1}$$

Where Q^{FA} the anode is volumetric flow rate, N_i^{DA} is the molar flow of species i in the anode diffusion layer, C_T is the total concentration, x_i^{FA} is the mole fraction of species i at the inlet of the anode channel, x_i^A is the mole fraction of species to the anode outlet channel. In the equations of the model, flows are regarded wonderful in the route from the anode to the cathode. The mass transport for methanol (1) and water (2) in the diffusion layers and response (DA and CA, respectively) Figure1, and considers each diffusion transport mechanisms by way of convection. In this model, it is assumed that the convection time period is due to the transport of water, ie, the consumption of water at the anode catalyst layer, and the permutation water via the membrane, [10, 11].

Therefore, the molar go with the flow charge of methanol and water via the diffusion layer and the anode catalyst layer can be expressed as.

$$N_i = -A_{cell} D_i^{L,eff} C_T \frac{dx_i}{dz} + x_i \left(\frac{I_{cell}}{6F} + N_2^M \right), \quad i = 1, 2 \tag{2}$$

Where A_{cell} the surface of the reaction zone, $D_i^{L,eff}$ is the effective diffusion coefficient of species *i* in the anode layers (liquid phase), I_{cell} is the current density, F is the Faraday constant, z is the axial coordinate and x_i the mole fraction of species *i*.

With regard to oxygen (3), carbon dioxide (4) and nitrogen (5) transport mechanisms in these areas are diffusion and convection. However, for these species, the constant regular of Henry's Law H_i is integrated in the convective term, due to the fact it is assumed that the dissolved gasoline merchandise [12]. As a first approximation, the solubility of species i in pure water was once used as the awareness of the methanol feed move is very low [1].

$$N_i = -A_{cell} D_i^{L,eff} C_T \frac{dx_i}{dz} + p_i^A H_i \left(\frac{I_{cell}}{6F} + N_2^M \right), \quad i = 3,4,5 \tag{3}$$

where p_i^A is the partial pressure (strain) of species i in the anode.

$D_i^{L,eff}$ the effective diffusion coefficient of species i in the diffusion layers and the anode response can be derived from the mass diffusion,, D_i^L coefficient and porosity of the two layers D_A^{DA} and D_A^{CA}, using the correction Bruggeman [13, 14].

$$D_i^{L,eff} = (\varepsilon_A)^{3/2} D_i^L \tag{4}$$

On the different hand, the consumption of water and methanol and formation of carbon dioxide additionally happens in the anodic response layer. Therefore, in steady of the conditions state, the change in this molar flow of species *i* is affected through the velocity of the anodic electrochemical response as follows:

$$\frac{dN_i^{CA}}{dz} = \nu_{1,i} \frac{i_A}{6F}, \quad i = 1,2,4 \tag{5}$$

Where i_A exchange local current in the anode and $\nu_{1,i}$ is the coefficient for a stoichiometric of species *i* at the reaction 1 (Figure 1).

The concentration between interfaces (AFC/ADL) and (ADL/ACL) given our have assuming local equilibrium with two coefficients K1 and K2, respectively.

to $x = x_1$ $\quad C_j^{ADL} = K_1 C_j^{AFC}$ j is methanol or water

to $x = x_2$ $\quad C_j^{ACL} = K_2 C_j^{ADL}$ j is methanol or water

B. Proton exchange membrane

As in the past mentioned, the butts of this work is the prediction of overall performance in the DMFC the use of parameters such as proton conductivity, swelling and permeability coefficients got by way of conventional characterization methods. [8]. As in traditional DMFC models, it is assumed that water and permeates methanol thru the membrane due to the electro-osmotic drag (convective term, ensuing of the cell cutting-edge density) and the concentration gradient of the species (diffusive term: resulting from the separate hydration nation of the membrane).

The species of electro-osmotic drift is assumed to be driven through the concentration gradient of [15] protons and parameterized by means of the wide variety of water transport, and the proton conductivity (obtained by means of impedance spectroscopy). The number of water transport is assumed to be the equal as that for Nafion® [16]. The proton concentration gradient is set in the DMFC by means of steam and swelling as described in [15, 11]. Furthermore, the diffusion time period is set via the permeability coefficient evaluated by means of pervaporation experiments [8]: this parameter is an approximation of the hydraulic permeability of the membrane [11, 17]. Therefore, the transport of water and methanol thru the membrane was expressed in the form:

$$N_i^M = -n_{drag,i} \frac{RTk_M}{F^2} \frac{dx_{H^+}^M}{dz} - A_{cell} P_i \frac{dx_i^M}{dz}, \quad i = 1,2 \tag{6}$$

Noted R is a gas constant, T is temperature operating t, x_i^M is a fraction mole of species i by the membrane and $x_{H^+}^M$ is the fraction mole of protons in the membrane.

Regarding the transport by the oxygen, carbon dioxide and nitrogen through the membrane, it is also assumed each mechanism of diffusion and convection. However, for these species, convection is superimposed by way of the float of water in the membrane. In addition, as for the anode regions, it is assumed that the transport of these species through the

membrane takes place as dissolved gases and therefore Henry's steady was once protected in the convection term. The diffusion term is set the use of coefficients of permeability measured by way of gasoline permeation experiments:

$$N_i^M = H_i p_i^M N_2^M - A_{cell} P_i \frac{dx_i^M}{dz} \quad , i = 3,4,5 \tag{7}$$

Using the parameters evaluated by using popular characterization strategies to simulate penetration of protons and all different species, is an approximation, when you consider that the authentic values for DMFC operation rely on running stipulations throughout the total MEA. In real operation of DMFC species awareness and protons in each (anode and cathode) varies with the utilized load and, therefore, distinct prerequisites exist in mass switch as in contrast to these in the traditional techniques of characterization such as impedance spectroscopy, pervaporation and gasoline switching.

The concentration between interface (ACL/M) and (M/CCL) given oure have assuming local equilibrium with two coefficient K3 and K4, respectively.

to $x = x_3$ $C_j^M = K_3 C_j^{ACL}$ j is methanol or water

to $x = x_4$ $C_j^{CCL} = K_4 C_j^M$ j is methanol or water

C. Cathode

Reduction of oxygen: $O_2 + 4H^+ + 4e^- \rightarrow 2H_2O$

Oxidation of methanol: $CH_3OH + \frac{3}{2}O_2 \rightarrow CO_2 + 2H_2O$

The oxygen transport process from the fuel tank and water are described as follows.

$$N_i^{DC} = Q^{FC} C_T \left(y_i^{FC} - y_i^C \right) \tag{8}$$

Where Q^{FC} is the volumetric rate flow at the cathode, N_i^{DC} is the flow molar for the species *i* in the diffusion layer cathode, y_i^{FC} is the mole fraction gas species *i* in a cathode, and y_i^C is the mole fraction gas species *i* in cathode outlet.

The Fick's diffusion approximation is used to represent the transportation of masses of all species in the gasoline segment via the diffusion layers and the cathode response (DC and CC, respectively), as shown in Figure 1.

$$N_i = -A_{cell} C_T D_i^{G,eff} \frac{dy_i}{dz} \tag{9}$$

Where $D_i^{G,eff}$ represents the species i's effective diffusion coefficient in the gas phase of the cathode layers.

By reducing oxygen and oxidizing the parasite methanol in the cathode reaction layer, species i is consumed and created there. As a result, in steady state, the electrochemical reactions of the cathode in this case have the following effects on the change in molar flow rates:

$$\frac{dN_i^{CC}}{dz} = \frac{1}{C_T A_{cell} 6F} \left(v_{2,i} i_C + v_{3,i} i_{MeOH} \right) \tag{10}$$

where i_{MeOH} is the parasitic exchange current resulting from methanol's interaction with the cathode catalyst layer, i_C the cathode's proton exchange density, N_i^{CC} is the species i molar flow in the cathode catalyst layer.

Given is the concentration at interfaces (CDL/CCL) and (CFC/CDL) under the assumption of a two-coefficient local equilibrium, K4 and K5, respectively.

to $x = x_5$ $C_j^{CDL} = K_5 C_j^{CCL}$ j is methanol or water

to $x = x_6$ $C_j^{CFC} = K_6 C_j^{CDL}$ j is methanol or water.

2.2. Electrochemical Kinetics

A. anode

Butler-Volmer can be used to calculate the rate of the electrochemical reaction at the anode catalyst layer [10]. The Tafel equation in terms of the concentration of methanol is simplified in this article.

$$i_A(z) = i_{A,ref}\left(\frac{x_1^{CA}(z)C_T}{C_{1,ref}^{CA}}\right)^{\gamma_A}\exp\left(\frac{\alpha_A F}{RT}\eta_A\right) \tag{11}$$

where $i_{A,ref}$ is the proton exchange repository of the anode's methanol oxidation-induced current density, x_1^{CA} is the mole fraction of methanol local, $C_{1,ref}^{CA}$ is the molar concentration of methanol repository, α_A is the charge transfer ratio, is overvoltage local anode and γ_A is the order of the chemical reaction for the oxidation of methanol in the anode.

The thickness of the catalyst layer is integrated across the local volumetric reaction rate. l_C , allows us to have the overall current density $I_A^{overall}$:

$$I_A^{overall} = \int_0^{l_C} i_A(z)\,dz \tag{12}$$

During the operation of the DMFC, there will be a change in the local overvoltage (voltage drop) due to the losses associated with the conduction of protons in the electrolyte and electrons in the solid phase. Consequently, the following equation can be used to determine the overall voltage drop in the anode catalyst layer:

$$\eta_A^{overall} = \frac{1}{I_{cell}}\int_0^{l_C} i_A(z)\eta_A(z)\,dz \tag{13}$$

Table 1 provides more specific details regarding the kinetic parameters that were employed.

B. Cathode

For both the oxygen reduction reaction and the methanol oxidation parasite, the electrochemical reactions at the cathode are also modeled using the Tafel equation [10]:

$$i_C(z) = i_{C,ref}\left(\frac{p_3^{CC}(z)}{p_{3,ref}^{CC}}\right)^{\gamma_C}\exp\left(-\frac{\alpha_C F}{RT}\eta_C\right) \tag{14}$$

$$i_{MeOH}(z) = i_{MeOH,ref}\left(\frac{C_1^{CC}(z)}{C_{1,ref}^{CC}}\right)^{\gamma_{MeOH}}\exp\left(-\frac{\alpha_{MeOH} F}{RT}\eta_{MeOH}\right) \tag{15}$$

Where $i_{C,ref}$ is the repository for proton exchange current density caused by the decrease in oxygen in the cathode, p_3^{CC} is the partial pressure of oxygen, $p_{3,ref}^{CC}$ is the reference oxygen partial pressure, α_C is the cathode's charge transfer coefficient, η_C is the locally elevated cathodic voltage, γ_C is how the chemical process for reducing oxygen in the cathode occurs, $i_{MeOH,ref}$ is the reference exchange current density of protons for the cathode side of methanol oxidation, $C_{1,ref}^{CC}$ is the cathode's reference molar concentration of methanol, C_1^{CC} is the amount of methanol in molar form at the cathode, α_{MeOH} also known as the charge transfer coefficient, η_{MeOH} Does the side reaction cause the voltage loss, γ_{MeOH} is how the related chemical reaction will occur.

Assessing the cathodic current density $I_C^{overall}$ the voltage dropped $\eta_C^{overall}$ Equations similar to equations (12) and (13) were used to accomplish these calculations over the cathode catalyst layer. On the other hand, the application $I_{MeOH}^{overall}$ of Faraday's law was used to assess the loss of the overall current density caused by the methanol oxidation reaction in the cathode catalyst layer:

$$I_{MeOH}^{overall} = N_1^M 6F \tag{16}$$

Overvoltage loss associated with cross-methanol $\eta_{MeOH}^{overall}$ was obtained using the Tafel equation to zero for the reaction [17]:

$$\eta_{MeOH}^{overall} = -\frac{RT}{\alpha_{MeOH} F} \ln\left[\frac{I_{MeOH}^{overall}}{I_{MeOH,ref}}\right] \tag{17}$$

is the reference current density for the cathode catalyst layer's methanol reaction.

2.3. Cell voltage

The battery voltage in an open circuit (OCV) produces the DMFC output voltage (OCV), U_{cell}^{0}, anode assembly and cathode over voltage protection, oxygen and methanol reactions, and ohmic loss caused by PEM resistance and contacts between the plates, electrodes, and membrane. [10]. The proton conductivity of the membrane as determined by impedance spectroscopy is used to calibrate the ohmic loss caused by PMEs. So, the following formula can be used to calculate the cell voltage:

$$U_{cell} = U_{cell}^{0} - \eta_{A}^{overall} + \eta_{C}^{overall} + \eta_{MeOH}^{overall} - \frac{d_M}{k_M} I_{cell} - R_{contact} I_{cell} \tag{18}$$

where is the thickness of the proton exchange membrane and is the DMFC contact resistance.

Where $R_{contact}$ is the DMFC contact resistance, and d_M what is the proton exchange membrane thickness.

The open circuit voltage was first estimated to be computed by subtracting the standard DMFC voltage (1.21V) from the voltage loss brought on by the functioning of the open circuit under methanol binding circumstances. [5]. As a result, we must anticipate the highest OCV value while utilizing a membrane with almost zero methanol permeability $\eta_{MeOH}^{overall} \cong 0$. Due to the voltmeter's non-idealities (usually $I_{cell} \le 1 mA/cm^2$), a current flow from the anode to the cathode when the OCV (experimental measurements) is conducted). In a perfect world, measuring the open circuit voltage would involve extending an infinite resistance. Although it is known that genuine voltmeters have a limited resistance ($R_v > 10 M\Omega$), some current can still pass through them. Therefore, a membrane with a proton conductivity very low may exhibit a substantial ohmic loss, which reduces the OCV's usefulness. Experimentally, this has frequently been confirmed for membranes with significant inorganic alterations. To account for the ohmic drop caused by the use of multilayer membranes with worse electrolyte characteristics, we used a current density $0.1 mA/cm^2$ of for open circuit conditions (based on the experimental test with the applied voltage meter). For the DMFC running at open circuit, surges of anodes and cathodes obtained from $\eta_{A}^{overall}$ and $\eta_{C}^{overall}$, respectively, evaluated by the expression Butler-Volmer rates, are negligible under the assumption of this current density. (Almost no reactions take place besides the parasitic methanol oxidation in the cathode catalyst layer).

2.4. Cells efficiency

The permeability of the membrane to methanol has a significant impact on the DMFC's efficiency. Methanol is permuted from the anode to the cathode through the PEM, which encourages methanol oxidation at the cathode and results in a potential loss. Additionally, it causes the reagents to be lost, which lowers the yield of DMFC. Typically, potentials and Faraday efficiency can be used to calculate DMFC efficiency [19]. The ratio of the current obtained from processed fuel (anode) to the total amount of processed fuel (anode plus cathode) is known as the Faraday efficiency. Consequently, the following equation provides it:

$$\eta_F = \frac{I_{celle}}{I_{MeOH}^{overall} + I_{celle}} \tag{19}$$

On the other hand, the potential effectiveness is calculated using the following equation as the voltage of the DMFC over the voltage of the standard cell due to the potential loss of assembly:

$$\eta_P = \frac{U_{cell}}{U_{cell}^{overall}} \tag{20}$$

Finally, the following equation is used to determine the DMFC's η_{DMFC} overall efficiency:

$$\eta_{DMFC} = \eta_P \eta_F \tag{21}$$

Table 1. Parameter values

Parameters	Value	References
U_{O_2}	$1.24\ V$	[21]
U_{CH_3OH}	$0.03\ V$	[21]
$\partial E / \partial T$	$-1.4\times10^{-4}\ (V/K)$	[22]
K	$0.036\ (\mathrm{S/cm})$	[21]
δ^{M}	$0.018\ (\mathrm{cm})$	[21]
$\delta^{AFC}, \delta^{CFC}$	$0.20\ (\mathrm{cm})$	assumed
$\delta^{ADL}, \delta^{CDL}$	$0.015\ (\mathrm{cm})$	assumed
$\delta^{ACL}, \delta^{CCL}$	$0.0023\ (cm)$	assumed
$\varepsilon^{AD}, \varepsilon^{CD}$	0.71	assumed
ε^{AC}	0.81	assumed
ε^{CC}	0.86	assumed
a	$1000\ (\mathrm{cm^{-1}})$	[21]
$I_{0,ref}^{CH_3OH}$	$9.425\times10^{-3}\exp\left((35570/R)(1/353-1/T)\right)\ (A/cm^2)$	[22]
$I_{0,ref}^{O_2}$	$4.222\times10^{-6}\exp\left((73200/R)(1/353-1/T)\right)\ (A/cm^2)$	[22]
k	7.5×10^{-4}	[21]
λ	$2.8\times10^{-9}\ (mol/cm^3)$	[21]
α_A	0.52	[21]
α_C	1.55	[21]
K_{1-2}	0.8	assumed
K_{5-6}	1.25	assumed
K_{3-4}	0.001	assumed
q^{AFC}	$0.33\ (\mathrm{cm^3/s})$	Real value
q^{CFC}	$1.67\ (\mathrm{cm^3/s})$	Real value
$n_{canales}$	15	Real value
L	$5\ (\mathrm{cm})$	Estimated
P_{air}	$1\ (atm)$	[23]
T_{AFC}	$343\ (K^0)$	Real value
T_{CFC}	$293\ (K^0)$	Real value
$D_{O_2}^{eff,CD,CC}$	$\varepsilon^{CD,CC^{2.5}}\left[\left(T^{1.75}\times5.8\times10^{-4}\right)/(27.772\times P)\right]\ (cm^2/s)$	[25]
$D_{O_2}^{eff,CFC}$	$\left[\left(T^{1.75}\times5.8\times10^{-4}\right)/(27.772\times P)\right]\ (cm^2/s)$	[25]
$D_{CH_3OH}^{AFC}$	$\left[\left(7.608\times10^{-7}\times T\right)/\left(\mu_{H_2O}\times9.485\right)\right]\ (cm^2/s)$	[25]
$D_{CH_3OH}^{eff,AD,AC}$	$\varepsilon^{AD,AC^{2.5}}\left[\left(7.608\times10^{-7}\times T\right)/\left(\mu_{H_2O}\times9.485\right)\right]\ (cm^2/s)$	[25]
$D_{CH_3OH}^{eff,CC}$	$\varepsilon^{CC^{2.5}}\left[\left(T^{1.75}\times5.8\times10^{-4}\right)/(33.904\times P)\right]\ (cm^2/s)$	[25]
$D_{CH_3OH}^{eff,M}$	$4.9\times10^{-6}\exp\left(2436\times(1/333-1/T)\right)\ (cm^2/s)$	[21]
$D_{H_2O}^{AFC}$	$\left[\left(6.295\times10^{-7}\times T\right)/\left(\mu_{CH_3OH}\times5.833\right)\right]\ (cm^2/s)$	[16]
$D_{H_2O}^{eff,AD,AC}$	$\varepsilon^{AD,AC^{2.5}}\left[\left(6.295\times10^{-7}\times T\right)/\left(\mu_{CH_3OH}\times5.833\right)\right]\ (cm^2/s)$	[25]
$D_{H_2O}^{eff,CD,CC}$	$\varepsilon^{CD,CC^{2.5}}\left[\left(T^{1.75}\times6.2\times10^{-4}\right)/(25.523\times P)\right]\ (cm^2/s)$	[25]
$D_{H_2O}^{eff,M}$	$2.0\times10^{-6}\exp\left(2060\times(1/303-1/T)\right)\ (cm^2/s)$	[25]
ξ_{CH_3OH}	$2.5\times x_{CH_3OH}$	[25]
n_d	$2.9\exp\left(1029\times(1/333-1/T)\right)\ (cm^2/s)$	[22]
K^{M}	$0.0043\ (\mathrm{W/cm.K})$	[25]
K^{AD}	$1.95+6.57\times10^{-4}\mathrm{T}\ (\mathrm{W/m.K})$	[25]
K^{CD}	$1.71+2.96\times10^{-5}\mathrm{T}\ (\mathrm{W/m.K})$	[25]
K^{AC}	$\left(1-\varepsilon^{AC}\right)\times86.7+\varepsilon^{AC}\left(0.341+9.26\times10^{-4}\right)\ (\mathrm{W/m.K})$	[25]
K^{CC}	$\left(1-\varepsilon^{CC}\right)\times71+\varepsilon^{CC}\left(0.0034+7.60\times10^{-5}\right)\ (\mathrm{W/m.K})$	[25]

3. Results and discussion

Simple digital tools and original Pro.8 fortran.90 were used to swiftly apply the model created for the passive DMFC power. Examples of model predictions are provided in this section. [21]. The parameters chosen to construct the simulations are the same ones the authors employed in their experiments [21]. Similar to passive DMFC systems, the temperature rises over time as a result of electrochemical processes, reducing the fuel cell yield. To show the effect of the latter on the performance of DMFC temperature was varied within a limited range of 390 to 395 K^0, K^0 is giving the graph of current density vs. voltage for each given temperature. The following, we will discuss the results of written fortran.90 software.

3.1. Methanol concentration curves

The methanol concentration profiles predicted through the anode and the membrane, are shown in Figure 2, when the cell is supplied with a methanol solution 0.5 (M) of current densities 15, 35 *et* 55 (mA/cm^2). Due to the fact that methanol diffuses by natural convection during the analysis period, the concentration profile at the methanol reservoir in the anode slightly drops near the interface with the diffusion layer (see equation (1)). Due to mass transfer diffusion, methanol consumption in the catalyst layer, and methanol crossing through the membrane to the cathode side, the concentration of methanol drops in the other layers.

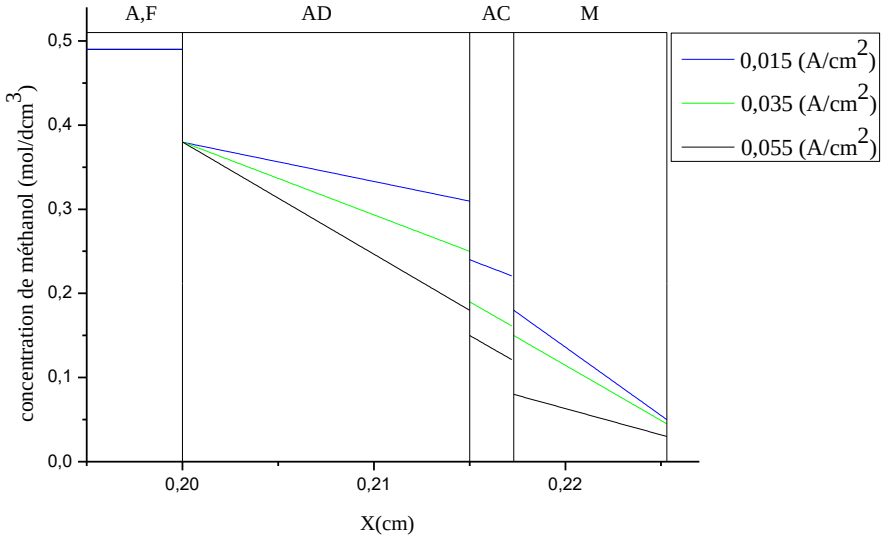

Figure 2. shows the projected methanol concentration patterns for various current densities using a 0.5M methanol solution

The rate of recovery of methanol in the membrane decreases with increasing current density, as can be observed from the plot of the concentration profile in which the membrane is depicted in this figure. As previously indicated, when methanol crosses a membrane, it combines with oxygen on the cathode side, creating a mixture of potential and an eddy current. The parasite known as current leaking current causes a fuel shortage. According to equation (24), the methanol crossings can be represented in terms of a current leakage, which suggests a better understanding of the effect of the methanol crossover's loss of efficiency.

As seen in Figure 3, the current of leakage increases with rising methanol concentration and falling current density, which is to be expected. By operating the cell at concentrations lower than 0.44 (M) methanol and higher current densities, the current that leaks and therefore methanol penetration can be decreased 15, 35 *et* 55 (mA/cm^2) and it was found that the results are enhanced and methanol crossover which is summarized in the methanol tank that permeate the membrane and tends worm zero (negative value) for different values of0.015(mA/cm^2) and0.035(mA/cm^2) ,and in a very clear way 0.055(mA/cm^2) .

In Figure 4 and to more improve the results of the current density was increased to 0.065(mA/cm^2), it is found that the difference negligible. While the results are a preferred current density is much expected that as a value by optimizing it the great value of 0.055(mA/cm^2) which 0.065(mA/cm^2), affects the transport of water and we will shout a flood in the membrane as will see the following.

Figure 5 illustrates the model predictions for the propagation coefficient of pure water dependent on the current intensity for various methanol concentrations. The concentration of methanol has a significant impact on the crossing of water, as shown by the locations (values of). It should be emphasized that positive values represent net water flow between the anode to the cathode, whilst negative values represent net flux generated on the opposite side.

Figure 5 for all tested methanol concentration values 0.20(*M*), 0.30(*M*), 0.40(*M*), 0.50(*M*) 0.60(*M*). Although lower readings being produced by utilizing high methanol concentrations, values are positive.

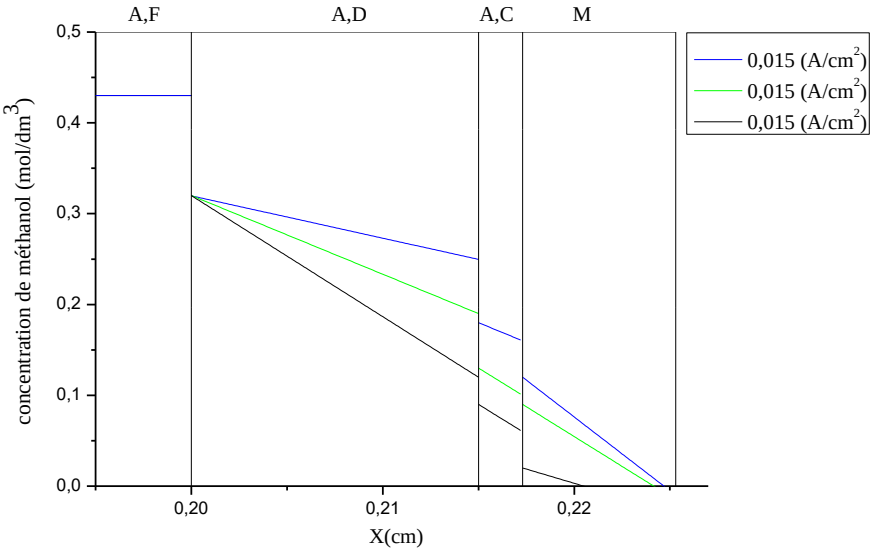

Figure 3. Using a 0.44 M methanol solution, projected profile of methanol concentration inside the cell for various current densities

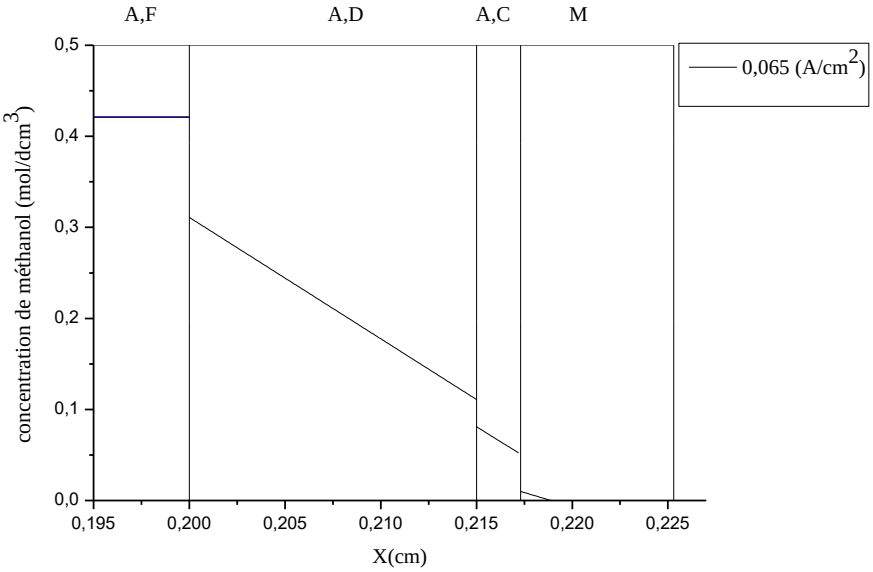

Figure 4. anticipated profiles of the cell's methanol concentration at a certain current density and 0.44 M methanol solution

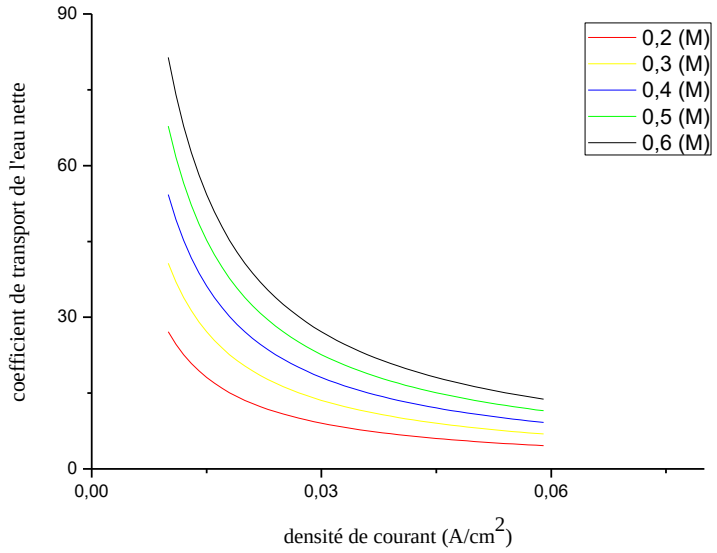

Figure 5. The model predictions for the transport coefficient of pure water at different concentrations of methanol

This can be explained by the fact that larger water concentrations on the side of the anode result from lower methanol feed concentrations. Water is largely carried to the cathode because there is a bigger difference in water content between the anode and cathode sides. Water is generated on the cathode side with concentrations above this side,

while smaller quantities of water are put in on the anode side at higher methanol concentrations. In this instance, the anode to cathode water transfer is still dominating (positive), However, because the gradient in water concentration is lower, less water is moved from the anode region to the opposite side of the cathode that corresponds to lesser values. It follows that the values are significantly influenced by the methanol content.

The model described in this article correctly predicts the trends of the impact of the concentration of methanol on the net water transportation coefficient. These trends are in line with what the authors have suggested.

3.2. Polarization curves

The temperature strongly affects the yield of the fuel cell. Figures-6-7-8-9-show the effect of this temperature on a DMFC using a composite membrane MEAs made from Poly (vinylidene fl uoride-hexa fluorine opropylene) (PVdF-HFP) / Nafion ionomer / oxy aluminum hydroxide, and concentrations (0.5 (*M*), 1(*M*), 1.5 (*M*), 2(*M*)) of methanol at various temperatures of 323 (K^0), 333 (K^0), 343 (K^0), 353 (K^0). The increase in temperature due to the chemical kinetics of the reactants of the fuel cell showed a significant increase in overall performance.

Figure 6 shows the polarization curve of a polyacrylamide membrane (vinylidene fl uoride-hexa fluorine opropylene) (PVdF-HFP) / Nafion ionomer / aluminum oxy hydroxide with 0.5 (M) of methanol and also with increasing temperatures. Although performance is improved more and showed similar results. Figures 7-9 show that as the operating temperature increases, it increases the methanol reactions with higher concentrations. This implies that the methanol crossover is more important at higher methanol concentrations and temperature. The increase in temperature allows more than protonation in the catalyst which increases performance, but at the same time allows a greater chance of having methanol crossover (Jung et al.) [15], these results show that there is a more consistent performance when the fuel cell's operating temperature and the methanol content are in equilibrium.

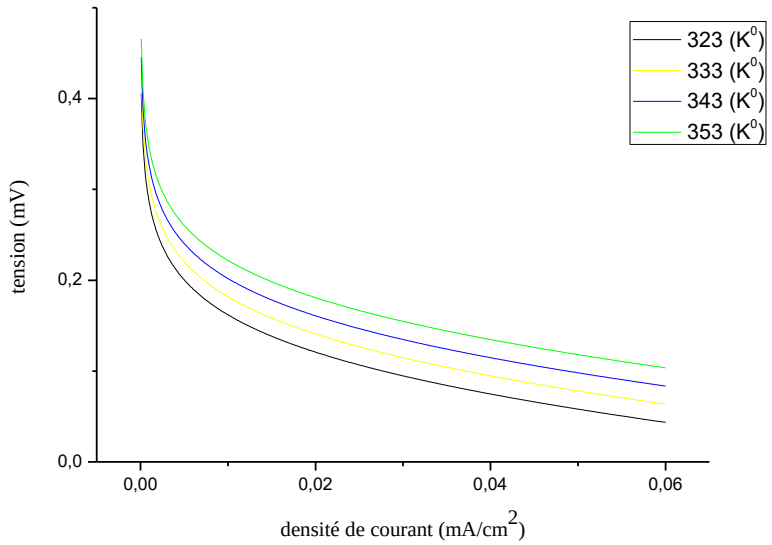

Figure 6. Different operating temperatures to methanol concentration 0.5 mol

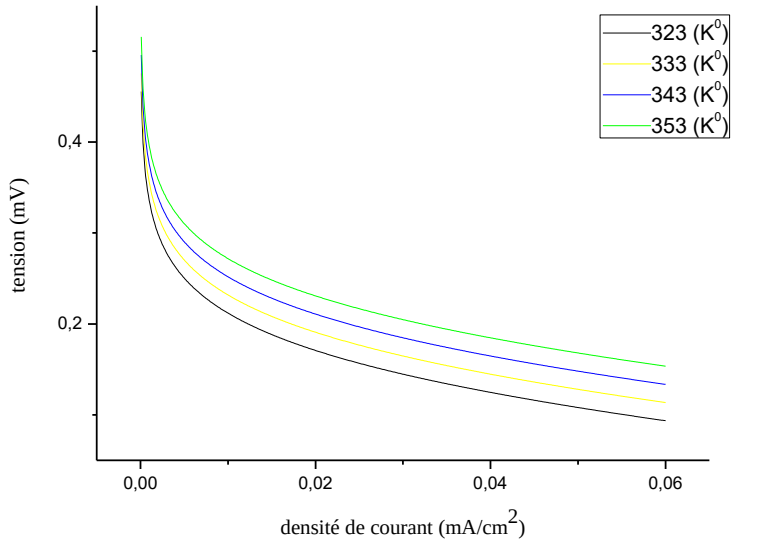

Figure 7. different operating temperatures to methanol concentration 1 mol

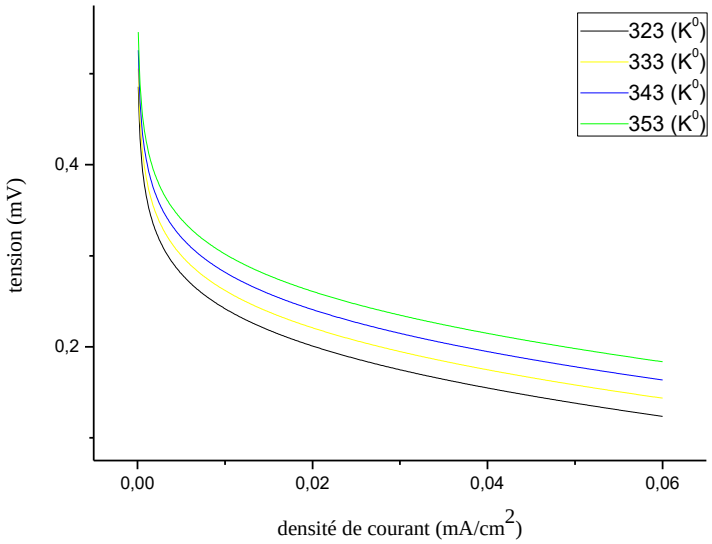

Figure 8. different operating temperatures to methanol concentration 1.5 mol

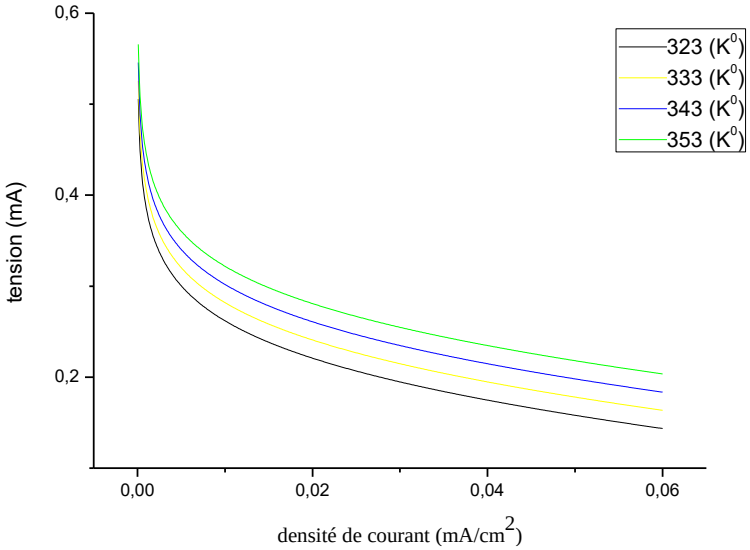

Figure 9. different operating temperatures to methanol concentration 2 moles

4. Conclusions

In this research, a steady state, a single-dimensional multi-component, and thermal model is provided in an effort to comprehend the operation of a passive DMFC and the important parameters on its performance as well as to create an efficient passive DMFC system.

The model predicts the effect of the operating conditions (such as methanol concentration and fuel cell temperature) and current density on the fuel cell performance and on water and methanol crossover

We conclude that in a range of and we will have the best conditions for the ideal function of a fuel cell-type DMFC.

For a value of we can prevent the appearance of methanol crossover phenomenon that breaks most of time of function the **leakage** current and decreases the ideal performance of DMFC.

Considering that the largest concentration of methanol decrease allows to have the flooding of the membrane which hinders the transmission of protons and consequently it leads to poor DMFC performance that's why we can consider that the value of is the most correct value that can be taken into consideration

As it has been seen in the sections before, net water transport coefficient increases with the decrease of the concentration of methanol, and so that remains a positive value that is to say, the water will be transported from the anode to the cathode, we defined the range of this value as the following where we consider that is limited in this range.

The increase of temperature means that the concentration of methanol is very high. While this temperature allows the smooth function of DMFC when it vaporizes water i.e it decreases the alpha value and on the other hand with the existence of a higher methanol consultation we will have the emergence of cross-over phenomenon again. Thus, we have to set the interval of this temperature in which DMFC can have the greatest efficiency without cross-over of methanol and for

The current simulator will be applied to study and create membranes. In addition, future research will focus on a thorough analysis of the PEM's characteristics for use in DMFCs, taking consideration the connection between water's permeability and diffusion, as well as the temperature of the cathode's (catalyst layer) side.

Nomenclature

α	Surface area of the anode, (cm^{-1})
A_α	Active surface, (cm^2)
A_1	Total area without holes, (cm^2)
A_{holes}	Total area of the holes, (cm^2)
C	Concentration, (mol/cm^3)
C_1	AFC / ADL interface concentration, (mol/cm^3)
C_2	ADL / LCD interface concentration, (mol/cm^3)
C_3	LCD / M interface concentration, (mol/cm^3)
C_4	M / CCL interface concentration, (mol/cm^3)
C_5	CCL / CDL interface concentration, (mol/cm^3)
C_6	CDL / CFC interface concentration, (mol/cm^3)
$C_{O2,ref}$	Oxygen reference concentration, (mol/cm^3)
C_P	Specific heat capacity, $(J/mol.K)$
$\partial E/\partial T$	Rate of change of the electromotive power, (V/K)
D	Diffusion coefficient, (cm^2/s)
D^{eff}	Effective diffusion coefficient, (cm^2/s)
E_{cell}	Potential thermodynamic equilibrium, (V)
F	Faraday's constant, $96500(C/mol)$
G	The Gibbs free energy, (J/mol)
g	Acceleration of gravity, (cm^2/s)
H	Enthalpie de réaction, (J/mol)
h_{mass}	Mass transfer coefficient, (cm/s)
h_{heat}	Heat transfer coefficient, (W/cm^2K)
I_{cell}	Current density of the cell, (A/cm^2)
I_{CH_3OH}	Leakage current density due to methanol crossover, (A/cm^2)
$I_{0,ref}^{CH_3OH}$	Exchange current density of methanol, (A/cm^2)
$I_{0,ref}^{O_2}$	Exchange current density of oxygen, (A/cm^2)
j_A	Volumetric current density, (A/cm^3)
k	Rate expression constant, (Eq. (27))
K_{2-8}	Partition coefficients
K	Thermal conductivity, (W/cm^2K)
L	Length of the active surface, (cm)
n_d	Electroosmotic drag coefficient of water
N	Molar flow, $(mol/cm^2.s)$
P_{air}	The pressure of the air in the cathode, (atm)
R	Gas constant,8.314 $(J/mol.K)$
R_{cell}	Internal resistance of the fuel cell, (cm^2/S)
R_{cond}	Conduction resistance, (K/W)
R_{conV}	Convection resistance, (K/W)
R_{total}	Total thermal resistance, (K/W)
T	Temperature, (K)
U_{CH_3OH}	Potential for thermodynamic equilibrium of the oxidation of methanol, (V)
U_{O_2}	Potential for thermodynamic equilibrium of the oxidation of oxygen, (V)
V_{cell}	Cell voltage, (V)
x_{CH_3OH}	Mole fraction of methanol,
x	Coordinate direction normal to the anode, (cm)

Greek letters

Δ	Variation
α	Transport coefficient of the net water
α_A	Anodic transfer coefficient
α_C	Cathodic transfer coefficient
δ	Thick, (cm)
ε	Porosity
η	Overvoltage, (V)
K	The ionic conductivity of the membrane, (S/cm)
λ	Constant in the expression rate (Eq. (27)), (mol/cm^3)
μ	Dynamic viscosity, $(g/cm.s)$

v	Kinematic viscosity, (cm^2/s)
ρ	Density, (g/cm^3)
v_{O_2}	The stoichiometric coefficient of oxygen in the cathode reaction
U_{H_2O}	The stoichiometric coefficients of water in the cathode reaction
v_{cross,O_2}	The stoichiometric coefficient of oxygen in the cathode reaction undesirable
v_{cross,H_2O}	The stoichiometric coefficients of water in the cathode reaction undesirable
ξ_{CH_3OH}	Electro-osmotic coefficient of drag of methanol

Indices

A	anode
C	cathode
CH_3OH	methanol
i	species *i*
j	species *j*
H_2O	water
O_2	oxygen

Exposants

0	feeding conditions
AFC	anode flow channel
ADL	layer anodically
ACL	anode catalyst layer
M	membrane
CCL	cathode catalyst layer
CDL	layer of cathodic diffusion
CFC	cathode flow channel

References

[1] S. Hietala, K. Koel, E. Skou, M. Elomaa and F. Sundholm, Thermal stability of styrene grafted and sulfonated proton conducting membranes based on poly (vinylidene fluoride), J. Mater. Chem. 8(1998) 1127. DOI：10.1039/A708288F

[2] Q. Ye, T.S. Zhao, A natural-circulation fuel delivery system for direct methanol fuel cells, Journal of Power Sources, 147 (2005) 196-202. DOI：10.1016/j.jpowsour.2005.01.026

[3] Y.H. Pan, Advanced air-breathing direct methanol fuel cells for portable applications, Journal of Power Sources 161 (2006) 282–289. DOI：10.1016/j.jpowsour.2006.03.048

[4] V. B.Oliveira, D. S. Falcao, C. M. Rangel and A. M. F.R. Pinto, "A comparative study of approaches to direct methanol fuel cells modeling," International Journal of Hydrogen Energy, vol. 32, pp. 415-424, 2007. DOI：10.1016/j.ijhydene.2006.06.049

[5] Y. Chiu, T. L. Yu and Y. Chung, "A semi-empirical model for efficiency evaluation of a direct methanol fuel cell", Journal of Power Sources, 2011. DOI：10.1016/j.jpowsour.2011.01.084

[6] J. G. Liu, T. S. Zhao, Z. X. Liang, R. Chen, Effect of membrane thickness on the performance and efficiency of passive direct methanol fuel cells, Journal of Power Sources 153 (2006) 61–67. DOI：10.1016/j.jpowsour.2005.03.190

[7] B.K. Kho, B. Bae, M. A. Scibioh, J. Lee, H.Y. Ha, On the consequences of methanol Crossover in passive air-breathing direct methanol fuel cells, Journal of Power Sources, 142 (2005) 50-55. DOI：10.1016/j.jpowsour.2004.10.027

[8] T.S. Zhao, R. Chen, W.W. Yang, C. Xu, Small direct methanol fuel cells with passive supply of reactants, Journal of Power Sources 191 (2009) 185–202. DOI：10.1016/j.jpowsour.2009.02.033

[9] B.L. García, V.A. Sethuraman, J.W. Weidner, R.E. White, Mathematical Model of a Direct Methanol Fuel Cell, Journal of Fuel Cell Science and Technology, Vol.1 November 2004 43-48. DOI：10.1115/1.1782927

[10] S. H. Seo and C. S. Lee, "A study on the overall efficiency of direct methanol fuel cell by methanol crossover current," Applied Energy, vol. 87, pp. 2597-2604, 2010. DOI：10.1016/j.apenergy.2010.01.018

[11] Thorsten Schultz, Experimental and Model-based Analysis of the Steady-state and Dynamic Operating Behaviour of the Direct Methanol Fuel Cell (DMFC), PhD

[12] R.C.Reid, J.M. Prausnitz, T.K. Sherwood, The Properties of Gases and Liquids,McGraw-Hill, 1977.

[13] V.B.Oliveira, D.S.Falcão, C.M. Rangel and A.M.F.R. Pinto, Modelling and experimentalstudies on a Direct Methanol Fuel Cell working under low methanol crossover and high methanol concentrations, International Journal of Hydrogen Energy, 34, 6443-6451. DOI：10.1016/j.ijhydene.2009.05.114

[14] K.Broka and P.Ekdunge, Oxygen and hydrogen permeation properties and water Uptake of Nafion 117 membrane and recast film for PEM fuel cell, Journal of Applied Electrochemistry 27 (1997) 281-289. DOI：10.1023/A:1018469520562

[15] K. Lee, J.H. Nam, J.H. Lee, Y. Lee, S.M. Cho, C.H. Jung, H.G. Choi, Y.Y. Chang, Y.U. Kwon and J.D. Nam, Methanol and proton transport control by using layered double hydroxide nanoplatelets for direct methanol fuel cell, Electrochemistry Communications, 7 (2005) 113–118. DOI：10.1016/j.elecom.2004.11.011

[16] M. A. Delavar, M. Farhadi and K. Sedighi, "Numerical simulation of direct methanol fuel cells using lattice Boltzmann method," International Journal of Hydrogen Energy, vol. 35, pp. 9306-9317, 2010. DOI：10.1016/j.ijhydene.2010.02.126

[17] P. Argyropoulos, K. Scott and W.M. Taama, Gas evolution and power performance in direct methanol fuel cells, Journal of Applied Electrochemistry 29(1999) 661-669. DOI：10.1023/A:1003589319211

[18] P. Argyropoulos, K. Scott and W.M. Taama, Carbon dioxide evolution patterns in direct methanol fuel cells, Electrochimica Acta 29 (1999) 661-669. DOI：10.1016/S0013-4686(99)00102-4

[19] J. Ko, P. Chippar and H. Ju, "A one-dimensional, two-phase model for direct methanol fuel cells - Part I: Model development and parametric study," *Energy*, pp. 2149-2159, 2010. DOI：10.1016/j.energy.2010.01.034

[20] Y. Wang, G. Au, E. J. Plichta, and J. P. Zheng, "A semi-empirical method for electrically modeling of fuel cell: Executed on a direct methanol fuel cell," Journal of Power Sources, vol. 175, pp. 851-860, 2008. DOI：10.1016/j.jpowsour.2007.09.101

[21] J. Zou, Y. He, Z. Miao and X. Li, "Non-isothermal modeling of direct methanol fuel cell," International Journal of Hydrogen Energy, vol. 35, pp. 7206-7216, 2010. DOI：10.1016/j.ijhydene.2010.01.123

[22] Y. Chiu, "An algebraic semi-empirical model for evaluating fuel crossover fluxes of a DMFC under various operating conditions," International Journal of Hydrogen Energy, vol. 35, pp. 6418-6430, 2010. DOI：10.1016/j.ijhydene.2010.03.080

[23] S. Basri and S. K. Kamarudin, "Process system engineering in direct methanol fuel cell," International Journal of Hydrogen Energy, pp. 1-18, 2011. DOI：10.1016/j.ijhydene.2011.02.058

[24] B. Xiao and A. Faghri, "Numerical analysis for a vapor feed miniature direct methanol fuel cell system," International Journal of Heat and Mass Transfer, vol. 52, pp. 3525-3533, 2009. DOI：10.1016/j.ijheatmasstransfer.2009.03.009

[25] M. Vera, "A single-phase model for liquid-feed DMFCs with non - Tafel kinetics," Journal of Power Sources, vol. 171, issue. 2, pp 763-777, 2007. DOI：10.1016/j.jpowsour.2007.05.098

[26] M.A. Abdelkareem, N. Nakagawa, DMFC employing a porous plate for an efficient operation at high methanol concentrations, Journal of Power Sources 162 (2006)114–123. DOI：10.1016/j.jpowsour.2006.07.012

[27] R. Chen, T.S. Zhao, J. G. Liu, Effect of cell orientation on the performance of passive direct methanol fuel cells, Journal of Power Sources 157 (2006) 351–357. DOI：10.1016/j.jpowsour.2005.07.073

[28] Y.H. Chan, T.S. Zhao, R. Chen, C. Xu, A self-regulated passive fuel-feed system for passive direct methanol fuel cells, Journal of Power Sources 176 (2008) 183–190. DOI：10.1016/j.jpowsour.2007.10.050

[29] B. Xiao, A. Faghri, Transient modelling and analysis of a passive liquid-feed DMFC, International Journal of Heat and Mass Transfer 51 (2008) 3127-3143. DOI：10.1016/j.ijheatmasstransfer.2007.08.022

[30] J. Liu, T.S. Zhao, R. Chen, C.W.Wong, Effect of methanol concentration on passive DMFC performance, Fuel Cells Bulletin (2005) 12–17. DOI：10.1016/S1464-2859(05)00521-3

[31] G. Jewett, A. Faghri, B. Xiao, Optimization of water and air management systems for a Passive direct methanol fuel cell, International Journal of Heat and Mass Transfer 52 (2009) 3564-3575. DOI：10.1016/j.ijheatmasstransfer.2009.03.006

[32] B. Xiao, H. Bahrami and A. Faghri, "Analysis of heat and mass transport in a miniature Passive and semi passive liquid-feed direct methanol fuel cell," Journal of Power Sources, vol. 195, pp. 2248-2259, 2010. DOI：10.1016/j.jpowsour.2009.10.047